CHEMISTRY
A EUROPEAN JOURNAL

DOI: 10.1002/chem.200800914

X–X Through-Cage Bonding in Cu, Ni, and Cr Complexes with M_3X_2 Cores (X = S, As)

Rosa Carrasco,[a, b] Gabriel Aullón,[a] and Santiago Alvarez*[a]

Abstract: Density functional calculations on trinuclear complexes bridged by two sulfur atoms, $[(tmeda)_3Cu_3(\mu\text{-}S)_2]^{3+}$, $[(tmeda)_3Ni_3(\mu\text{-}S)_2]^{2+}$, and $[(tmeda)_3Ni_3(\mu\text{-}S_2)]^{4+}$, as well as on the formation of $[(tmeda)_3Cu_3(\mu\text{-}S)_2]^{3+}$ from a dinuclear $[(tmeda)_2Cu_2(\mu\text{-}S_2)]^{2+}$ complex and a mononuclear $[(tmeda)Cu(\eta^2\text{-}S_2)]^{+}$ fragment, are reported. A qualitative orbital analysis of the M_3X_2 framework bonding is presented for the case in which each metal atom M has a square planar coordination sphere completed by one bidentate or two monodentate ligands (that is, $[(L_2M)_3X_2]$ compounds). It is concluded that a framework electron count (FEC) of 12 corresponds to systems with six M–X bonds but no X–X bond through the cage, while an FEC of 10 favors the formation of an X–X bond. Framework electron counting rules are also presented for related M_3X_2 cores in $[(L_5M)_3X_2]$ complexes, based on a qualitative molecular orbital (MO) analysis supported by DFT calculations on $[(OC)_{15}Cr_3(\mu\text{-}As_2)]$.

Keywords: bridging ligands · copper · density functional calculations · framework electron counting · sulfur

Understanding the structural preferences and redox properties of sulfur-bridged polynuclear copper complexes is relevant to copper–sulfur active sites, such as the Cu_Z site in nitrous oxide reductase,[1] cupredoxins,[2] or metallothioneins,[3] considering their importance in several biological processes. In research devoted to this purpose, Tolman and coworkers recently reported the reaction of β-diketiminato Cu^{II} complexes with $(tms)_2S$ (tms:bis(trimethylsilyl)), or of a Cu^{I} analogue with S_8, to yield disulfido Cu^{II} complexes **1a** with a short S–S bond length.[4] Similar complexes have been obtained by Itoh and coworkers by reaction of Cu^{II} species with sodium disulfide.[5] X-ray absorption spectroscopy and DFT computational studies by the Solomon group on a related trispyrazolylborate-capped dinuclear complex have shown the high covalency and delocalization of the unpaired electrons in the Cu_2S_2 core.[6] Related dicopper(II) complexes with an end-on bridging disulfide group have been reported by Karlin and coworkers.[7] To the best of our knowledge, all structurally characterized dinuclear copper compounds with unsubstituted bridging sulfur atoms forming a Cu_2S_2 ring have similar structures, with S–S < 2.22 Å.

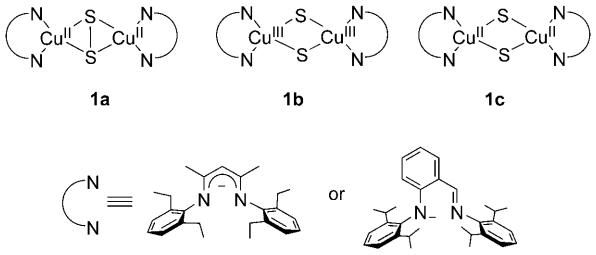

Concerned about the possibility of breaking the S–S bonds in such complexes, we searched in a computational study for alternative chelating ligands that could favor such a task and yield a molecular structure **1b**. In spite of the variety of model compounds tried, we were unable to obtain a single example with the bis(sulfido) bridging structure **1b**, and only two-electron reduction could be proposed as a way to obtain an open structure **1c**.[8] Such a structure was later reported by Delgado et al.; it was obtained through a serendipitous reaction in which the sulfides are generated by C–S bond cleavage from dipyridyl disulfide.[9]

[a] Dr. R. Carrasco, Dr. G. Aullón, Prof. S. Alvarez
Departament de Química Inorgànica and
Institut de Química Teòrica i Computacional (IQTC-UB)
Universitat de Barcelona, Martí i Franquès 1–11
08028 Barcelona (Spain)
Fax: (+33)
E-mail: santiago@qi.ub.es

[b] Dr. R. Carrasco
Current address: IFIC (CSIC-Universitat de València)
Apt. Correus 22085, 46071 València (Spain)

Supporting Information for this article (atomic coordinates of the title complexes and other relevant structural information) is available on the WWW under http://dx.doi.org/10.1002/chem.200800914.

Tolman and coworkers carried out a similar reaction of a dicopper(I) complex bearing substituted ethylenediamine ligands **2** with S_8, and obtained instead trinuclear complexes **3**

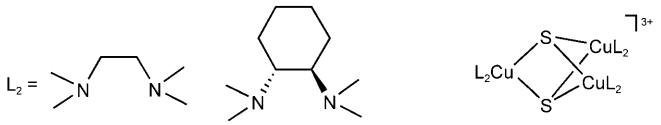

2

3

with $\{Cu_3S_2\}^{3+}$ cores and long S–S bond lengths (2.69–2.72 Å).[10] Preliminary computational studies on such compounds allowed us to understand why they present a delocalized triplet ground state, in contrast to an oxo-bridged analogue,[10] which is asymmetric with one Cu^{III} and two ferromagnetically coupled Cu^{II} ions. In the present work we report detailed computational studies on a possible pathway for the formation of the trinuclear compound by reaction of a dinuclear disulfido-bridged Cu^{II} complex with a mononuclear Cu^{I} one. We then endeavor to provide a qualitative orbital model for describing the M–X and X–X bonding in complexes with similar M_3X_2 cores, using a delocalized MO scheme similar to the framework electron counting rules developed earlier for the simpler M_2X_2 skeletons. Those rules have been very successful in interpreting the existence or nonexistence of through-ring M–M or X–X bonds.[11,12] To test the qualitative predictions of the framework electron count rules, we then report calculations on trinuclear complexes with $\{Ni_3S_2\}^{2+}$ and $\{Ni_3S_2\}^{4+}$ cores. Analysis of bonding in the related family of compounds with $\{(L_5M)_3X_2\}$ cores (M = Mo, W; X = As, Sb, Bi)[13] and bonding X–X lengths requires consideration of the different orbital topology of their L_5M fragments. Therefore, in the last section we present a qualitative MO analysis and the resulting rules for the framework electron count (FEC), supported by DFT calculations on $[(OC)_{15}Cr_3(\mu\text{-}As_2)]$.

Abstract in Spanish: *En este artículo se presentan cálculos basados en la teoría del funcional de la densidad (DFT) para complejos trinucleares con dos átomos de azufre puente, $[(tmeda)_3Cu_3(\mu\text{-}S)_2]^{3+}$, $[(tmeda)_3Ni_3(\mu\text{-}S)_2]^{2+}$ y $[(tmeda)_3Ni_3(\mu\text{-}S_2)]^{4+}$, así como para la reacción de formación del primero de ellos a partir del compuesto dinuclear $[(tmeda)_2Cu_2(\mu\text{-}S_2)]^{2+}$ y de un fragmento mononuclear $[(tmeda)Cu(\eta^2\text{-}S_2)]^{+}$. Se propone un análisis orbital cualitativo del enlace en el esqueleto M_3X_2 para el caso en que cada átomo metálico M tenga una esfera de coordinación plano cuadrada, en complejos del tipo $[(L_2M)_3X_2]$. Se concluye que un número de electrones de esqueleto (FEC) igual a 12 corresponde a sistemas con seis enlaces M–X y sin enlace X–X, mientras que un FEC de 10 favorece la formación de un enlace X–X. Se presentan también las reglas de recuento de electrones de esqueleto para los grupos M_3X_2 en complejos $[(L_5M)_3X_2]$, basadas en un análisis de orbitales moleculares cualitativo, corroborado por cálculos DFT para el compuesto $[(OC)_{15}Cr_3(\mu\text{-}As_2)]$.*

Results and Discussion

Formation of a trinuclear Cu_3S_2 complex: The main results of our DFT calculations for the mono-, di-, and trinuclear complexes $[(tmeda)Cu(\eta\text{-}S_2)]^{+}$, $[(tmeda)_2Cu_2(\mu\text{-}S_2)]^{2+}$, and $[(tmeda)_3Cu_3(\mu\text{-}S)_2]^{3+}$ (tmeda:tetramethylethylendiamine), as well as those for the transition state for the formation of the last of these, are reported in Table 1. The most relevant molecular structures are shown in Figure 1 and their atomic coordinates are supplied in the Supporting Information.

Mononuclear complex: The basic building block, a mononuclear fragment, was optimized with a side-on coordinated S_2 unit, $[(tmeda)Cu(\eta^2\text{-}S_2)]^{+}$. We found the calculation on this fragment of interest for our study of the formation of a trinuclear compound and the ligand exchange reactions. The coordination geometry of the complex in its triplet state can be described as trigonal planar with a η^2-S_2 coordinated group. The high spin density at the S_2 group (+1.51), close to the two spins expected for an independent neutral S_2 molecule, and the net charges (+0.97 for Cu, −0.28 for S_2) suggest a Cu^{I} formal oxidation state and a neutral paramagnetic disulfur ligand. However, an alternative Cu^{II}/S_2^{-} description cannot be ruled out, given the significant delocalization of the MOs carrying the unpaired electrons, as pointed out by a referee.

Dinuclear complex: The dinuclear compound could appear with the unpaired electrons at the copper atoms coupled either antiferro- (with a net molecular spin $S=0$) or ferromagnetically ($S=1$). We have therefore optimized this molecule in both its singlet and triplet states. The geometry of the closed-shell singlet state corresponding to the electron configuration represented in Figure 2 is in good agreement with the experimental structures of analogous diketiminate dinuclear complexes,[4] the average bond lengths (10 compounds) of which are S–S = 2.19(3), Cu–S = 2.21(2), and Cu–N = 1.91(1) Å. The energy of the triplet state is barely 1 kcal mol^{-1} above the singlet state at the computational level employed. An important observation is that the optimized Cu_2S_2 core of this molecule is planar in its singlet state, but significantly bent in the triplet state, with an angle between the two CuS_2 planes (θ) of 118°, indicating that coordination of the bridging sulfur atoms to a third copper atom requires only a relatively undemanding intersystem crossing from the planar singlet to the bent triplet state, which has already the geometry required for interaction with the incoming $Cu^{I}L_2$ fragment. The most significant changes from the mono- to the dinuclear complex are found at the S_2 bridge, with an increased negative charge and a drastically decreased spin density in the triplet state (Table 1). They indicate a partial reduction of the disulfur unit, approaching the $Cu^{I}Cu^{II}/S_2^{-}$ or $Cu^{II}Cu^{II}/S_2^{2-}$ formal de-

Table 1. Structural and population analysis (NBO) results for the optimized structures of $[(tmeda)Cu(\eta^2\text{-}S_2)]^+$ (Cu_1), $[(tmeda)_2Cu_2(\mu\text{-}S_2)]^{2+}$ (Cu_2), $[(tmeda)_3Cu_3(\mu\text{-}S)_2]^{3+}$ (Cu_3), and the transition state (TS) of the formation reaction.[a]

	Cu_1 (S=1)	Cu_2 (S=1)	Cu_2 (S=0)	TS (S=1)	TS (S=0)	Cu_3 (S=1)	Cu_3 (S=0)
structural data[b]							
Cu^A–S(μ_2)	–	2.352(2)	2.270	2.326(1)	2.343	–	–
Cu^A–S(μ_3)	–	–	–	2.525	2.46	2.349(1)	2.35(4)
Cu^B–S	2.351	–	–	2.301	2.321	–	–
S···S	2.164	2.135	2.202	2.179	2.213	2.594	2.665
Cu^A–N	–	2.065(1)	2.035	2.07(2)	2.07(2)	2.079(2)	2.080(2)
Cu^B–N	2.068	–	–	2.082(5)	2.09(4)	2.10(1)	–
θ [°]	–	118	180	116	117	120	118–123
charges							
Cu^A	–	+1.00	+0.99	+1.00	+0.94	+1.03	+1.03
Cu^B	+0.97	–	–	+0.90	+1.04	–	–
S_2 unit	−0.28	−0.72	−0.78	−0.97	−0.99	−1.32	−1.38
spin densities							
Cu^A	–	+0.34	0.0	+0.31	+0.36	+0.35	2(+0.31)/−0.40
Cu^B	+0.33	–	–	+0.21	−0.21	–	–
S_2 unit	+1.51	+0.94	0.0	+0.63	+0.08	+0.28	−0.35

[a] ESDs are given in parentheses for average values. [b] All distances are in Å.

scriptions of such compounds, although the delocalized nature of the framework MOs makes it sensible not to put much emphasis on consideration of the formal oxidation states. We discuss this issue below, with the wider perspective obtained from calculations on the trinuclear complex and the transition state.

Although the bent triplet structure has not been observed experimentally so far, its possible participation in the formation of trinuclear complexes makes its study interesting. First, we can explain the bent structure in the triplet state as a second-order Jahn–Teller distortion that allows mixing of the full and semi-occupied orbitals of B_{3u} and B_{1g} symmetries, as shown schematically for **4** in Figure 2. The structural differences between the planar singlet and the bent triplet states are also explained by the topology of the highest-occupied MOs: 1) the promotion of an electron from the nonbonding b_{1g} to the Cu–S antibonding $2b_{2g}$ orbital in the triplet state accounts for a significant increase in the Cu–S bond lengths (0.08 Å); 2) the smaller contribution of S–S π^* orbitals in $2b_{2g}$ than in b_{1g}, combined with the partial depopulation of b_{3u} through mixing with b_{1g}, accounts for the shortening of the S–S bond length in the triplet state. Finally, the strongly delocalized nature of the two SOMOs depicted in Figure 2 are responsible for the spread of the calculated spin density in the bent triplet state: 34% at the Cu, 47% at the S, and 18% at the N atoms. It must be noted that an open-shell singlet state with the $(b_{1g})^1(2b_{2g})^1$ configuration (see Figure 2) has also been optimized. As expected from its relationship with the triplet through a spin flip, its Cu_2S_2 core is bent and its geometry and charge distribution are quite similar to those of the triplet. This singlet state, however, is 0.4 kcal mol^{-1} (153 cm^{-1}) above the closed-shell singlet represented in Figure 2.

Transition state: The transition state for the addition of one $[Cu(tmeda)]^+$ unit to the dinuclear complex has been located both for the triplet and open-shell singlet (the atomic coordinates are provided as Supporting Information). The singlet transition state has been found to be nearly 3 kcal mol^{-1} (1022 cm^{-1}) higher than the triplet one, but their geometries and electronic structures are quite similar (Table 1). A relevant structural aspect of the transition state is that the S–S bond is practically unaffected by coordination to the third copper atom. Additionally, a nonbonding orbital (NBO) population analysis gives a more negative net charge for the S_2 unit than that in the dinuclear complex (Table 1), consistently with its further reduction toward a coordinated disul-

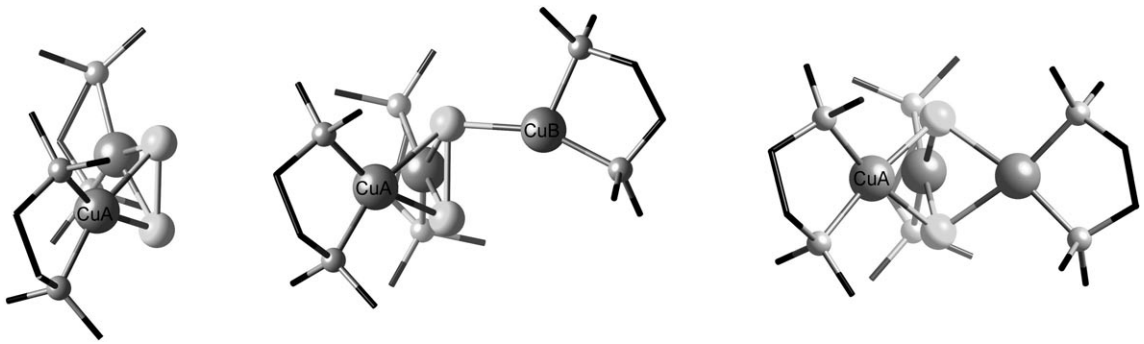

Figure 1. Optimized structures of the triplet state of the di- and trinuclear complexes $[(tmeda)_2Cu_2(\mu\text{-}S_2)]^{2+}$ (left), $[(tmeda)_3Cu_3(\mu\text{-}S)_2]^{3+}$ (right), and the transition state connecting them (center).

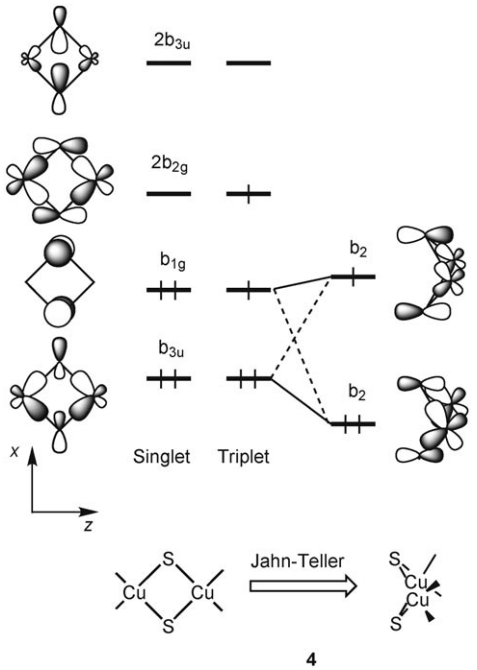

Figure 2. Schematic diagram of the framework orbitals of the dinuclear Cu_2S_2 core and its second-order Jahn–Teller distortion.

fide ion. The incoming copper atom (Cu^B in Figure 1) can be described formally at the transition state as a tricoordinated Cu^I ion, both from its trigonal planar geometry (sum of bond angles = 360°) and from its calculated charge. Therefore, other than the formation of one Cu–S bond with the mononuclear fragment and the weakening of the Cu–S bonds to the sulfur atom that becomes triple bridging, the starting dinuclear complex undergoes no major structural change.

Trinuclear complex: The trinuclear complex appears to be more stable in the triplet than in the singlet state (by 1520 and 1406 cm^{-1} in vacuum and in dichloromethane, respectively), in agreement with the experimental findings. Therefore, we discuss here only the results for the triplet state. On going from the transition state to the trinuclear complex, the most salient changes are 1) a significant increase of the S–S bond length, from 2.18 to 2.59 Å; 2) a corresponding increase in the S-M-S bond angles, from 53 to 67°; 3) a higher negative charge on the S_2 unit (from −0.97 to −1.32). All these data are consistent with the reduction of the disulfido bridge to two sulfide ions which would imply a formal two-electron oxidation of the entering Cu^I ion to Cu^{III} and its adoption of a square planar coordination. However, the system is highly delocalized and the three copper atoms are equivalent, with an average oxidation state of +2.33, as discussed in our preliminary communication.[10] It must be noted that the two unpaired electrons are delocalized through the three copper (atomic spin density of +0.35 each) and donor atoms (+0.14 at each S atom and +0.11 at each N donor atom).

To compare the optimized geometry with experimental data, we have retrieved from the Cambridge structural database (CSD) the S–S bond length and S-M-S bond angle for all di- and trinuclear transition metal complexes with M_3S_2 cores (Figure 3). Those data are clearly separated into two

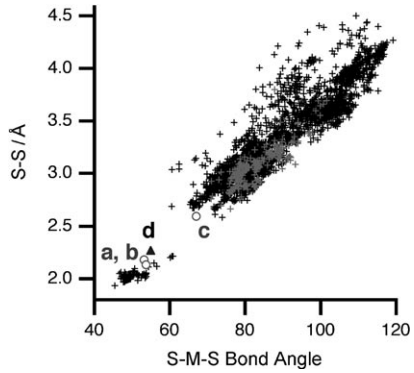

Figure 3. Calculated structural parameters (circles) associated with the S_2 fragment in di- and trinuclear complexes, $[(tmeda)_2Cu_2(\mu\text{-}S_2)]^{2+}$ (**a**, ○), and $[(tmeda)_3Cu_3(\mu\text{-}S)_2]^{3+}$ (**c**, ○), and in the transition state (**b**, ○) that connects them, compared with the corresponding experimental parameters found for all di- (black crosses) and trinuclear complexes (gray crosses) with S_2 bridges (with or without an S–S bond), as retrieved from the CSD. The optimized geometry of $[(tmeda)_3Ni_3(\mu\text{-}S_2)]^{4+}$ (**d**, ▲) is included.

groups: one with long S–S bond lengths and large S-M-S bond angles, another with short S–S bond lengths and small S-M-S angles. These two groups can be associated without problem to bis(sulfido)- and disulfido-bridged complexes, respectively. By comparison with the experimental data, the calculated S–S bond lengths and average S-Cu-S bond angles are consistent with the classification of the S_2 group in the dinuclear complex and in the transition state as a disulfide with short S–S bond lengths, whereas in the trinuclear compound they agree with the presence of two sulfido bridges. Whether or not the sulfur atoms should be considered as bonded in the trinuclear complex has been the subject of an intense debate with Hoffmann, Mealli, and coworkers, who propose the existence of some degree of bonding in spite of the relatively long bond length, based on the calculated occupation of the σ*(S–S) orbital.[14] The details of this debate will be published elsewhere.[15]

The reaction: In the gas phase, the transition state is calculated to be 68 kcal mol^{-1} above the independent di- and mononuclear complexes with the former in its triplet state. Given the minute structural changes on going from the dinuclear complex to the transition state, it is clear that the high activation energy is the result of the coulombic repulsion between the two positively charged fragments. Indeed, when the presence of a solvent is taken into account, the formation of the trinuclear complex is calculated to proceed with a much smaller barrier (1.3 kcal mol^{-1} in CH_2Cl_2) or even without an energy barrier (in water). Similarly, the formation of the trinuclear complex is calculated to be energet-

ically uphill (62.2 kcal mol^{-1}) in the gas phase, but favored thermodynamically by 9.5 and 18.2 kcal mol^{-1} in the presence of dichloromethane and water, respectively.

Replacement of the tmeda ligand in the optimized structure of the trinuclear complex by diketiminato ligands shows that substituents in the latter experience severe steric congestion when R = Me, Ph or 2,6-*i*Pr$_2$C$_6$H$_3$. Those substituents can be held at a nonrepulsive distance only if the two sulfur atoms remain bonded to each other and the copper atom at a correspondingly longer distance. This result of simple molecular modeling provides an explanation for why the diketiminato derivatives do not form a trinuclear complex but only a dinuclear one with a short S–S length.

Regarding the formal description of the two bridging sulfur atoms as S_2, S_2^-, or S_2^{2-} with a sulfur–sulfur bond, or as two sulfide ions with no bond, we think it is more interesting to focus on the whole series of mono- to trinuclear complexes (Table 1) rather than on each compound individually. We analyze the evolution of the net charge and total spin density at the S_2 group as the number of Cu–S bonds increases (Figure 4, top), and observe a monotonic increase in the negative charge and a decrease in spin density consistent with a gradual evolution from neutral S_2 (no net charge, spin density = 2.0) to monoanionic persulfide S_2^- (one negative charge, spin density = 1.0), to disulfide S_2^{2-} (two negative charges, zero spin density), to two sulfides (four negative charges, zero spin density). Interestingly, the same trend encompasses the neutral independent S_2 molecule and the bridging S_2 groups in the copper complexes. Whereas the trend is clear, the actual numerical values should be treated with care, given the significant mixing of sulfur and copper in the MOs relevant for S–S bonding. In particular, the contrast is important between the gradual change in the electronic characteristics of the disulfur bridge and the abrupt change in the S–S bond length (Figure 4, bottom), which varies little for compounds with two to five Cu–S bonds, but increases dramatically when an additional bond is formed in the trinuclear complex.

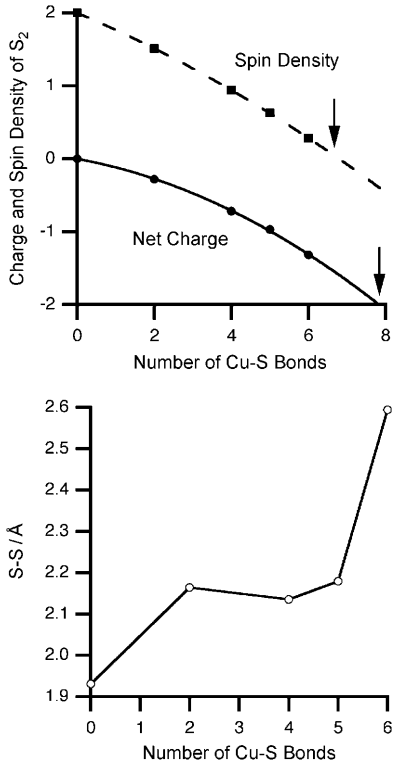

Figure 4. Top: Calculated net charge (circles) and spin density (squares and broken line) at the S_2 group in the free molecule and coordinated in copper complexes (Table 1) in their triplet states, as a function of the number of Cu–S bonds. The limiting case of two sulfide ions is indicated by arrows. Bottom: Evolution of the S–S distance in an S_2 group as a function of the number of Cu–S bonds it forms.

Framework orbital analysis for {(L$_2$M)$_3$X$_2$} cores: The S–S bonding in the Cu_3S_2 core of the trinuclear complex under study being intermingled perforce with the Cu–S bonding, a delocalized MO view of such a core is more adequate than an attempt to describe it based on two-center–two-electron Lewis structures. In this section we therefore present a qualitative orbital analysis of M_3X_2 cages of type **3**, following the guidelines of our earlier studies of bonding in simpler M_2X_2 rings.[11,12] We consider initially only those systems in which each metal atom bears either one bidentate or two monodentate terminal ligands (L_2) that, together with the two bridging atoms X, form an approximately square planar coordination sphere around each metal.

Our departure point is the assumption that a naked main group atom X in the triply-bridging position contributes three sp^3 hybrid orbitals to bonding within the M_3X_2 framework (**5**), while a fourth outward-pointing sp^3 hybrid holds a lone pair and is essentially M–X nonbonding (Figure 5). The location of two lone pairs away from the X···X region has been verified for the topologically and electronically related [1.1.1]propellane via an analysis of the electron localization function[16] (for a discussion on the analogy between this propellane and the M_3X_2 compounds, see below). Therefore, each of the two X atoms participates in the framework bonding with three lobes and $n-2$ electrons, where n is its number of valence electrons (that is, six electrons when X is a sulfide ion). A thiolate bridge would therefore be isolobal with a sulfide, contributing three sp^3 lobes and six electrons to framework bonding.

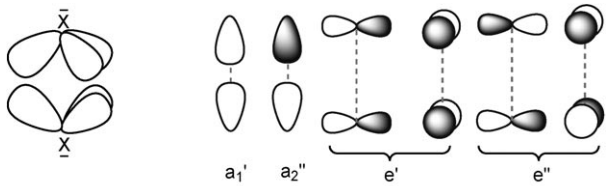

5 6

Figure 5. Orbitals of the X-bridging atoms contributing to framework bonding in M_3X_2 cages of type **3**.

Given the D_{3h} symmetry of the M_3X_2 skeleton, it is better to use symmetry-adapted versions of those lobes, taking combinations of the two bridging atoms, shown as **6** in Figure 5. Similarly, we consider the orbitals of L_2M fragments that can complete their square planar geometry with the two X ligands, each providing two lobes for bonding with the bridging ligands, which will be empty if the metal has eight valence electrons. The symmetry-adapted combinations of those orbitals, **7**, are shown in Figure 6.

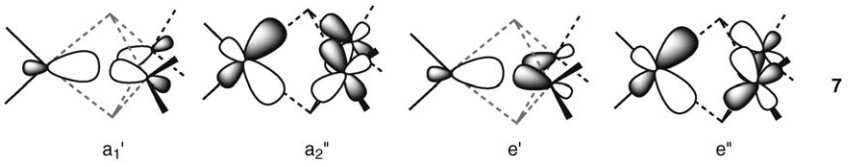

7

Figure 6. Symmetry-adapted combinations of the metal orbitals participating in framework bonding in M_3X_2 cages of type **3**.

By combining orbitals of the M_3 and X_2 fragments of the same symmetry (**6** and **7**), we can generate six M–X bonding and six M–X antibonding framework orbitals (Figure 7). Occupation of the six framework bonding orbitals with a total of 12 electrons would therefore account for six two-electron M–X bonds. In other words, leaving aside the electrons that do not participate in framework bonding (eight nonbonding valence electrons of each d^8 metal atom and the two outward-pointing lone pairs of the bridging atoms), we need the three metals and two bridging ligands to provide a total of 12 electrons in order to have optimum bonding for the M_3X_2 core. We may thus conclude that the framework electron count required for such a regular core is 12 (in short, FEC = 12), as in the hypothetical complex $[(tmeda)_3Ni_3(\mu\text{-}S)_2]^{2+}$ (see below).

Consider now the possibility of X–X bonding. Our orbital analysis indicates that the σ bonding orbital of the X_2 group is shared by the occupied and empty framework orbitals $1a_1'$ and $2a_1'$ (Figure 7) and should be roughly half occupied. Similarly, the antibonding $\sigma^*(X_2)$ combination is shared by the occupied $1a_2''$ and empty $2a_2''$ orbitals. If the net occupations of $\sigma(X_2)$ and $\sigma^*(X_2)$ are similar, the X–X bond order would be close to zero. Therefore, a reasonable description of the FEC = 12 complexes of type $[(L_2M)_3(\mu\text{-}X)_2]$ is similar to that shown in **3**, with six M–X bonds and no through-cage X–X bond. Consistently, more than 40 such compounds found in the CSD with a variety of metals, terminal ligands, and bridges (M = Ni, Pd, Pt, Rh, and Ir; X = NR, O, OH, S, SR, Se, or Te), and having the same electron count, present X···X lengths that are at least 0.5 Å longer than twice the atomic radius[17] of X (see the Supporting Information for details). For comparison, in all dinuclear complexes with a disulfido bridging ligand,[4,18] the S–S bond lengths exceed twice the sulfur covalent radius by at most 0.1 Å.

If we squeeze the M_3X_2 core to get the two X atoms closer, the $1a_2''$ orbital (Figure 7) is strongly destabilized, due to its $\sigma^*(X_2)$ contribution. What is required, then, to make a short X–X bond length possible is to empty that orbital by changing the total electron count: that is, by moving to a system with FEC = 10. Although we have found no examples of structurally characterized trinuclear complexes built up from d^8 square planar centers with this electron count, calculations on the hypothetical nickel compound $[(tmeda)_3Ni_3(\mu\text{-}S_2)]^{4+}$, reported below, suggest that such an architecture should be possible. A related reversible formation of a Te–Te bond upon two-electron oxidation of $[(PEt_3)_4Pt_2(\mu\text{-}Te)_2]$ is noteworthy,[19] but the corresponding oxidation of the analogous trinuclear complex, $[(PEt_3)_6Pt_3(\mu\text{-}Te)_2]^{2+}$, with FEC = 12, has not been reported.

Conversely, adding one more electron per metal atom would achieve a framework electron count of 15, partially occupying three framework antibonding orbitals ($2e''$ and $2a_2''$, Figure 7,

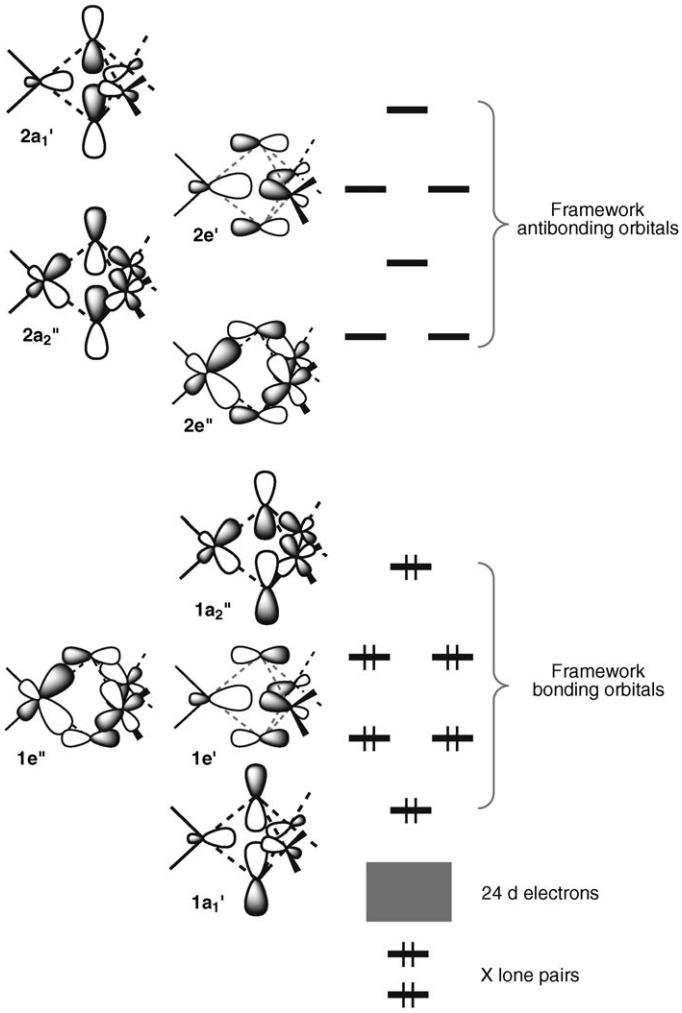

Figure 7. Schematic diagram for the framework orbitals of trinuclear complexes of d^8 square planar fragments forming M_3X_2 cores. For simplicity, only one orbital of each degenerate set is depicted; the orbital occupation shown corresponds to $[(tmeda)_3Ni_3(\mu\text{-}S)_2]^{2+}$.

with important contributions from the metal $d_{x^2-y^2}$ orbitals), as expected for three square planar (or severely Jahn–Teller distorted six-coordinate) Cu^{II} centers. In the case of the $[(tmeda)_3Cu_3(\mu\text{-}S)_2]^{3+}$ complex discussed above, FEC = 14 corresponds to a formal oxidation state of $Cu^{2.33+}$.

When we consider M_3X_2 cores in which the d^8 ML_2 fragments are replaced by other d^n ML_x fragments, we need to take into account how many nonbonding d electrons must be counted for such fragments and the nature of the metal orbitals available for framework bonding.[12,20] For instance, a d^6 ML_4 fragment would complete an octahedral coordination with the two bridging ligands, using the two empty orbitals **8** (Figure 8) for framework bonding. Two examples of

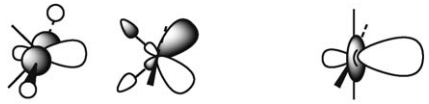

8 9

Figure 8. Acceptor orbitals of d^6 ML_4 (**8**) and d^6 ML_5 (**9**) fragments.

such systems found in the literature, with Os_3Se_2 and Co_3S_2 cores[21] and FEC = 12, show clearly nonbonding X–X lengths (3.22 and 2.95 Å, respectively). The different situation that appears when the metal fragment has only one orbital available for framework bonding, as in d^6 ML_5 groups (**9**), is discussed in a later section.

Another interesting system results when the three metal atoms are tetrahedrally coordinated, since in that case the five d orbitals become formally nonbonding,[22] and the metal atom employs sp^3 hybrids for bonding with the ligands. Thus, the same metal atom may hold eight or ten nonbonding electrons, depending on whether the orientation of the terminal ligands is coplanar with or perpendicular to the $M(\mu\text{-}X)_2$ unit and giving rise to an interesting series of isomers in the case of dinuclear systems with M_2X_2 cores.[8] Returning to trinuclear systems, we therefore expect optimum bonding within the framework for d^{10} ML_2 fragments to which the two bridges donate 12 electrons (that is, FEC = 12). This is the case for a Cu^I compound reported by Han et al.,[23] with two SH^- bridges, each of which provides six framework electrons, as well as for a related Ag^I compound with SH^- bridges.[24]

X–X bond formation in M_3X_2 complexes with FEC = 10: According to the MO scheme (Figure 7), a trinuclear compound with FEC = 10 should present a short X–X bond length, owing to the emptying of the $1a_2''$ orbital with significant σ*(X–X) character. To check this prediction, we have optimized the geometry of a trinuclear Ni complex in two different oxidation states, $[(tmeda)_3Ni_3(\mu\text{-}S)_2]^{2+/4+}$, corresponding to 12 and 10 framework electrons, respectively. The optimized structures are shown in Figure 9. As expected from the FEC rules discussed above, the $[(tmeda)_3Ni_3(\mu\text{-}S)_2]^{2+}$ cation, with FEC = 12, shows a long S–S bond

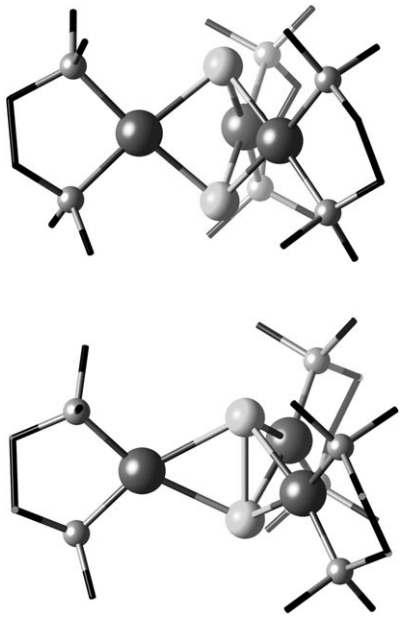

Figure 9. Optimized structures for the $[(tmeda)_3Ni_3(\mu\text{-}S)_2]^{2+}$ (top) and $[(tmeda)_3Ni_3(\mu\text{-}S_2)]^{4+}$ (bottom) cations with FEC = 12 and 10, respectively.

(2.87 Å). A two-electron oxidation of that complex results in the FEC = 10 analogue, $[(tmeda)_3Ni_3(\mu\text{-}S_2)]^{4+}$, with a short S–S bond length of 2.26 Å, and correspondingly longer Ni–S bonds (from 2.28 to 2.45 Å) owing to the Ni–S bonding character of the $1a_2''$ orbital that is emptied. Oxidation seems to affect mostly the bridging atoms, according to the population analysis, since the formal charge of −0.80 at each S atom drops to −0.56 while the charge on each Ni atom increases only slightly (from +0.82 to +0.90). There is a precedent for a bridge-centered oxidation accompanied by a shortening of the X–X bond in a Cu_2P_2 core,[25] which has been determined by X-ray absorption spectroscopy[26] and theoretical calculations.[27]

It is appropriate here to make a connection between the two Ni complexes shown in Figure 9 and purely organic analogues that result from isolobal analogies. Thus, formal replacement of the d^8 NiL_2 fragments with isolobal CH_2^{2+} and of sulfide ions by CR^{3-} ones converts $[(tmeda)_3Ni_3(\mu\text{-}S)_2]^{2+}$ into the neutral bicyclo[1.1.1]pentane (**10a**) with 12 framework electrons and a correspondingly long C–C bond length between the apical carbon atoms (1.86–1.91 Å in 26 structur-

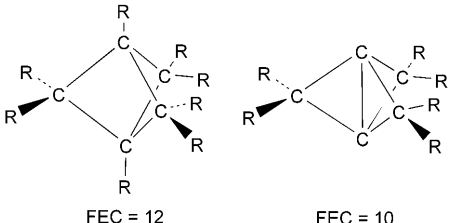

FEC = 12
1.88–1.91 Å
10a

FEC = 10
1.55–1.60 Å
10b

al data found in the CSD). If the apical atoms are replaced by two bare C^{3-} anions instead, these provide only five framework electrons each, keeping an outward-pointing lone pair.[16] Therefore, the total FEC is now 10, as in $[(tmeda)_3Ni_3(\mu\text{-}S_2)]^{4+}$, and the expected short distance between the apical carbon atoms corresponds with the molecular structure of [1.1.1]propellane (**10b**),[28] the derivatives of which have C–C distances between 1.55 and 1.60 Å (10 structural data found in the CSD).

Analysis of the electron density: To characterize further the electronic structure of the compounds studied, we analyzed the electron density $\rho(r)$ topologically for the optimized geometries of trinuclear complexes, within the framework of the atoms in molecules (AIM) theory.[29] A similar analysis of dinuclear species was reported earlier.[8] According to this theory, the main properties of the electron density can be summarized in terms of critical points. A bond critical point, also called a (3,−1) critical point, corresponds to two negative and one positive curvature of the electron density between two atomic nuclei and is taken as an indication of the presence of a chemical bond. Ring critical (3,+1) points are characterized by a single negative curvature and indicate a cyclic path of chemical bonds around it, and cage critical (3,+3) points with three positive curvatures correspond to a tridimensional cage of chemical bonds surrounding them.

For the trinuclear complexes analyzed, $[(tmeda)_3Cu_3(\mu\text{-}S)_2]^{3+}$, $[(tmeda)_3Ni_3(\mu\text{-}S)_2]^{2+}$, and $[(tmeda)_3Ni_3(\mu\text{-}S_2)]^{4+}$, the expected (3,−1) bond critical points for all M–S and M–N pairs have been found, consistently with the presence of single bonds, according to their ellipticities ($\varepsilon = 0.11$; see the Supporting Information). The positive values of $\nabla^2\rho(\mathbf{r})$ (0.12–0.14 for M–S and 0.30–0.38 for M–N bonds) point to shared interactions characteristic of donor–acceptor X–M bonds and indicate a higher covalent character for the M–S than for the M–N bonds.

The optimized structure of $[(tmeda)_3Ni_3(\mu\text{-}S)_2]^{2+}$ presents a (3,+3) cage critical point at the center of the Ni_3S_2 skeleton and no S–S bond critical point, consistently with an FEC = 12 system for which six Ni–S bonds and no S–S bond are expected, a situation analogous to that depicted in **3**. For each of the two other trinuclear complexes, $[(tmeda)_3Cu_3(\mu\text{-}S)_2]^{3+}$ and $[(tmeda)_3Ni_3(\mu\text{-}S_2)]^{4+}$, an extra (3,−1) bond critical point between the two sulfur atoms has been found, which might be indicative of S–S bonding. The difference between these two complexes, however, is that the electron density at the bond critical point is significantly lower in the copper (0.046) than in the nickel compound (0.084), consistently with the formal description of the latter as bearing an S–S bond. The existence of S–S bonding in the copper complex according to the AIM analysis, surprising as it may seem at first sight, could be the result of the different participation of the σ and σ*(S–S) combinations in the occupied framework orbitals. On the other hand, comparison of the AIM parameters calculated for the trinuclear Cu compound and those for simple S_2^{n-} species (Table 2) may cast some doubt on the real meaning of the existence of an S···S bond critical point. In fact, both the electron density at that critical point and its Laplacian have nearly identical values for the S···S contact within the copper complex and for two bare sulfide ions placed at the same distance.

Table 2. Results of the AIM analysis at the S···S bond critical points: total electron density, $\rho(\mathbf{r}_c)$, and Laplacian of the electron density, $\nabla^2\rho(\mathbf{r}_c)$.

	S···S [Å][a]	$\rho(\mathbf{r}_c)$	$\nabla^2\rho(\mathbf{r}_c)$
$[(tmeda)_3Cu_3(\mu\text{-}S)_2]^{3+}$	2.594	0.046	+0.112
$[(tmeda)_3Ni_3(\mu\text{-}S_2)]^{4+}$	2.256	0.084	+0.044
S_2	1.931	0.179	−0.213
S_2^-	2.060	0.138	−0.094
S_2^{2-}	2.281	0.089	+0.010
$(S^{2-})_2$	2.594	0.044	+0.105

[a] Optimized distances, except for $(S^{2-})_2$, for which the two sulfide ions were kept fixed at the value found in the copper complex.

In the light of the FEC rules, it is interesting that the electron density at the M–S bond critical points in the Ni compound with all framework bonding orbitals occupied (FEC = 12) is 0.078. Occupation of framework antibonding orbitals in the Cu compound (FEC = 14) results in a decrease in that electron density ($\rho(\mathbf{r}_c) = 0.066$) and a similar effect is observed when one framework bonding orbital is emptied in the reduced Ni complex ($\rho(\mathbf{r}_c) = 0.051$). Furthermore, $\rho(\mathbf{r}_c)$ for the M–S bonds shows an excellent negative linear correlation with the M–S bond lengths and a positive linear correlation with the S–S bond length. Thus, the variation of those three parameters with the framework electron count indicates that the FEC = 12 situation corresponds to the strongest M–S and weakest S–S bonding.

Framework electron counting for complexes with ML_5 fragments: In this section we analyze the similarities and differences in bonding within a M_3X_2 core when each metal atom has five peripheral ligands and formula $[(L_5M)_3(\mu\text{-}X)_2]$, which is represented schematically in **11**. A d^6 ML_5 fragment is isolobal with the CH_3^+ cation.[30] Each such fragment has one lobe available (that is, **9** for d^6 ML_5 as in Figure 8 or an sp^3 hybrid for CH_3^+) for an extra bond, and forms the electronically saturated d^6 XML_5 or XCH_3 species by interaction with a two-electron donor X. In that case, three of the symmetry-adapted combinations of the bridging atom orbitals in the M_3X_2 core (e″ and a_2''; see Figure 5) do not interact significantly with metal orbitals of the same symmetry, and the relevant MOs are as shown in Figure 10. This leaves only three MOs of M–X bonding character ($1a_1'$ and the degenerate pair 1e′). These orbitals also incorporate X–X σ ($1a_1'$) and π (1e′) bonding character. The optimum bonding between those five atoms is reached for systems that have 18 electrons at the metal d orbitals (corresponding to d^6 configura-

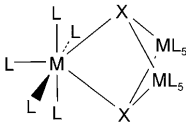

11

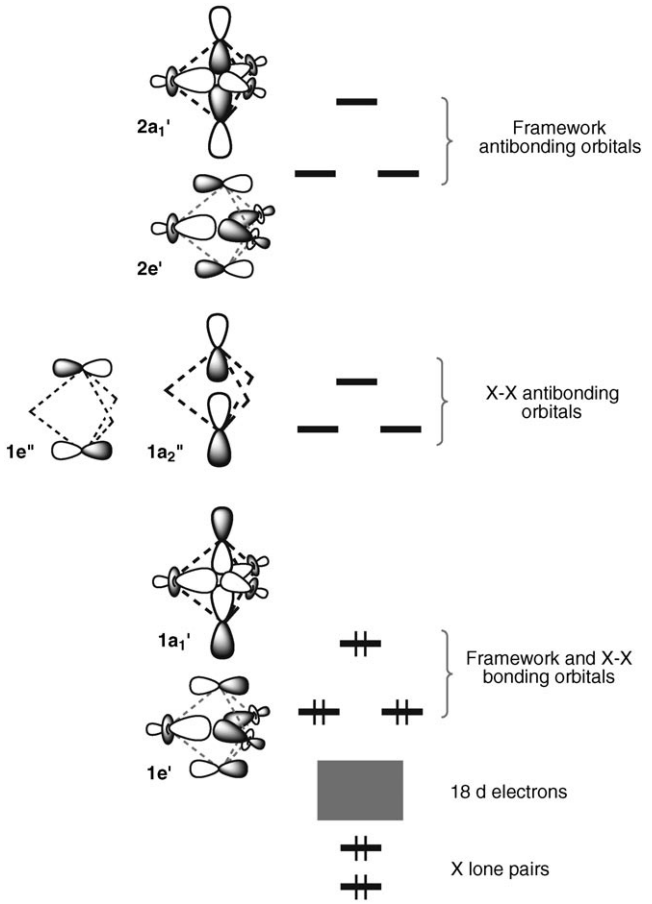

Figure 10. Qualitative diagram of the framework orbitals in trinuclear complexes of d^6 ML_5 fragments forming M_3X_2 cores. The orbital occupation shown corresponds to FEC = 6.

tions), four electrons for the outward-pointing X lone pairs, and six electrons occupying the framework and X–X bonding orbitals $1a_1'$ and $1e'$. This thus corresponds to FEC = 6.

The situation regarding X–X bonding is very different from that found above for the systems built up from d^8 ML_2 fragments. Even if the $\sigma(X_2)$ and $\pi(X_2)$ orbitals are delocalized throughout the M_3X_2 framework, their antibonding counterparts ($1a_2''$ and $1e''$) are empty, as required by their net antibonding character. Consequently, a formal X–X triple bond can be invoked appropriately.

The qualitative orbital scheme in Figure 10 is supported by the topology and relative energies of Kohn–Sham orbitals in DFT calculations performed for $[(OC)_{15}Cr_3(\mu\text{-}As_2)]$. In the optimized structure of that compound (atomic coordinates of which are provided as Supporting Information) the As–As bond length is short (2.246 Å), as predicted for its framework electron count of six. The through-ring distance is practically coincident with that found experimentally in the W analogue (2.278 Å).[31]

Other members of the family discussed here were synthesized in the 1980s by Huttner and coworkers.[13] $[(OC)_{15}W_3(\mu\text{-}Bi_2)]$ and $[\{(MeCp)(OC)_2Mn\}_3(\mu\text{-}Bi_2)]$ were structurally characterized. Electron counting can verify that all these compounds have an FEC of six, and the Bi–Bi distances close to 2.81 Å are consistent with the existence of X–X chemical bonds, by comparison with the sum of covalent radii of 2.96 Å.[17]

Conclusion

The $[(tmeda)_2Cu_2(\mu\text{-}S_2)]^{2+}$ dinuclear complex appears to have similar energies in its singlet state with a planar Cu_2S_2 core and in the bent triplet state. Its reaction with a mononuclear $[(tmeda)Cu]^+$ fragment to give the $[(tmeda)_3Cu_3(\mu\text{-}S)_2]^{3+}$ trinuclear complex is found to have a very low activation energy in the triplet energy surface. The S_2 unit in the copper complexes undergoes a gradual reduction as the number of bonded copper atoms increases, along the path $S_2 \rightarrow S_2^- \rightarrow S_2^{2-} \rightarrow (S^{2-})_2$. In contrast, the S–S bond length increases abruptly only after formation of the trinuclear complex. The FEC scheme for $[(L_2M)_3(\mu\text{-}X)_2]$ compounds indicates that optimum M–X bonding is achieved for FEC = 12, whereas for FEC = 10 systems weaker M–X bonds and a short X–X distance are to be expected. The results of geometry optimization for $[(tmeda)_3Ni_3(\mu\text{-}S)_2]^{2+}$ and $[(tmeda)_3Ni_3(\mu\text{-}S_2)]^{4+}$ and comparison with those for $[(tmeda)_3Cu_3(\mu\text{-}S)_2]^{3+}$ are in agreement with those predictions and with the results of a topological analysis of the electron density, which is nevertheless inconclusive regarding the bonding nature of the S–S interaction in the copper trinuclear complex.

Framework electron counting rules based on a qualitative MO analysis for related M_3X_2 cores formed by d^6 ML_5 fragments indicate that $[(L_5M)_3X_2]$ complexes have only three framework bonding orbitals and the optimum M–X and X–X bonding corresponds to an FEC = 6 case, for which a short X–X distance should be expected, consistently with a formal triple bond, thus providing a rationale for the structures of Huttner's compounds $[(OC)_{15}W_3(\mu\text{-}Bi_2)]$, $[(OC)_{15}W_3(\mu\text{-}As_2)]$, and $[\{(MeCp)(OC)_2Mn\}_3(\mu\text{-}Bi_2)]$.

Experimental Section

Computational methods: Unrestricted density functional calculations were carried out using the Gaussian 03 package,[32] with the B3LYP hybrid method that employs the Becke three-parameter exchange functional[33] and the Lee–Yang–Parr correlation functional.[34] An Ahlrichs all-electron triple-ζ basis set was used for the Cu, Ni, and Cr atoms,[35] supplemented with two polarization functions.[35,36] A similar basis set was used for the S and As atoms,[35] supplemented with an extra d-polarization function.[36] A double-ζ basis set was used for H, C, N, and O.[36] All optimized structures reported have been verified by vibrational analysis to be true minima or transition states. The influence of the dielectric environment provided by a solvent was studied using the nonequilibrium implementation of the polarizable continuum model in its conductor version (CPCM) when the medium is water (dielectric constant 78.39) or dichloromethane (8.93).[37] The evaluation of singlet–triplet energy gaps was carried out by nonprojected DFT calculations using the methodology described elsewhere.[38] For the topological analysis of the electron density, critical points have been generated with the Xaim routine.[39]

Structural analysis: Experimental structural data were retrieved from the Cambridge Structural Database (Version 5.29 with one update, January 2008)[40] and the Inorganic Crystal Structure Database (Release 2006-1).[41] A search for structures with $\{(L_2M)_3X_2\}$ cores was extended to all group 3–10 transition metals and to X atoms belonging to periodic groups 14–17 and restricted to trinuclear complexes with square planar coordination of the metal atom and unsubstituted bridging atoms X. A total of 49 fragments corresponding to 42 different chemical compounds were found, with M = Ni, Pd, Pt, Rh, or Ir, and X = O, S, Se, Te, or Cl, and X···X distances at least 0.3 Å greater than the sum of the atomic radii. A less restrictive search for S···S interactions in $\{M_2X_2\}$ and $\{M_3X_2\}$ cores (Figure 3) included all transition metals with any coordination number and geometry. A total of 2696 crystallographically independent fragments in 1953 structures were found for dinuclear complexes, in 82 of which S–S bond lengths were shorter than 2.22 Å while in the rest they were longer than 2.58 Å. For trinuclear complexes 238 fragments were found in 203 crystal structures, all of which had S–S distances longer than 2.66 Å.

Acknowledgements

Financial support to this work was provided by the Dirección General de Investigación Científica (MEC) through grant CTQ2005-08123-C02-02/BQU and by the Comissionat per a Universitats i Recerca (Generalitat de Catalunya) through grant 2005SGR-0036. The computing resources at the Centre de Supercomputació de Catalunya (CESCA) were made available in part through a grant from the Fundació Catalana per a la Recerca (FCR) and the Universitat de Barcelona. The authors thank W. Tolman for inspiring this study, helpful discussions, and a careful and critical reading of the manuscript. R. Hoffmann and C. Mealli are also acknowledged for thought-provoking discussions on the possible existence of S–S bonding in the trinuclear copper compound and for calling our attention to Huttner's systems and to propellane. Two anonymous referees are also acknowledged for suggesting the possibility of a persulfide character of the bridging unit in the mononuclear copper complex and for spotting some missing technical details.

[1] P. Chen, S. I. Gorelsky, S. Ghosh, E. I. Solomon, *Angew. Chem.* **2004**, *116*, 4224; *Angew. Chem. Int. Ed.* **2004**, *43*, 4132; S. Ghosh, S. I. Gorelsky, S. D. George, J. M. Chan, I. Cabrito, D. M. Dooley, J. J. G. Moura, I. Moura, E. I. Solomon, *J. Am. Chem. Soc.* **2007**, *129*, 3955.

[2] C. Dennison, *Coord. Chem. Rev.* **2005**, *249*, 3025; Y. Lu in *Comprehensive Coordination Chemistry II, Vol. 8* (Ed.: T. J. Meyer), Elsevier, Amsterdam, **2004**, p. 91.

[3] P. González-Duarte in *Comprehensive Coordination Chemistry II, Vol. 8* (Eds.: J. A. McCleverty, T. J. Meyer), Elsevier, Amsterdam, **2004**, p. 213.

[4] E. C. Brown, N. W. Aboelella, A. M. Reynolds, G. Aullón, S. Alvarez, W. B. Tolman, *Inorg. Chem.* **2004**, *43*, 3335; E. C. Brown, I. Bar-Nahum, J. T. York, N. W. Aboelella, W. B. Tolman, *Inorg. Chem.* **2007**, *46*, 486.

[5] M. Inosako, C. Shimokawa, H. Sugimoto, N. Kihara, T. Takata, S. Itoh, *Chem. Lett.* **2007**, *36*, 1306.

[6] R. Sarangi, J. T. York, M. E. Helton, K. Fujisawa, K. D. Karlin, W. B. Tolman, K. O. Hodgson, B. Hedman, E. I. Solomon, *J. Am. Chem. Soc.* **2008**, *130*, 676.

[7] M. E. Helton, P. Chen, P. P. Paul, Z. Tyeklár, R. D. Sommer, L. N. Zakharov, A. L. Rhenigold, E. I. Solomon, K. D. Karlin, *J. Am. Chem. Soc.* **2003**, *125*, 1160; D. Maiti, J. S. Woertink, M. A. Vance, A. E. Milligan, A. A. Narducci Sarjeant, E. I. Solomon, K. D. Karlin, *J. Am. Chem. Soc.* **2007**, *129*, 8882.

[8] G. Aullón, S. Alvarez, *Eur. J. Inorg. Chem.* **2004**, 4430.

[9] S. Delgado, A. Molina-Ontoria, M. E. Medina, C. J. Pastor, R. Jiménez-Aparicio, J. L. Priego, *Polyhedron* **2007**, *26*, 2817.

[10] E. C. Brown, J. T. York, W. E. Antholine, E. Ruiz, S. Alvarez, W. B. Tolman, *J. Am. Chem. Soc.* **2005**, *127*, 13752.

[11] P. Alemany, S. Alvarez, *Inorg. Chem.* **1992**, *31*, 4266; G. Aullón, P. Alemany, S. Alvarez, *J. Organomet. Chem.* **1994**, *478*, 75; X.-Y. Liu, A. A. Palacios, J. J. Novoa, S. Alvarez, *Inorg. Chem.* **1998**, *37*, 1202; A. A. Palacios, G. Aullón, P. Alemany, S. Alvarez, *Inorg. Chem.* **2000**, *39*, 3166; G. Aullón, S. Alvarez, *Inorg. Chem.* **2001**, *40*, 4937.

[12] S. Alvarez, A. A. Palacios, G. Aullón, *Coord. Chem. Rev.* **1999**, *185–186*, 431.

[13] G. Huttner, U. Weber, L. Zsolnai, *Z. Naturforsch., B: Chem. Sci.* **1982**, *37*, 707; K. Plossl, G. Huttner, L. Zsolnai, *Angew. Chem. Int. Ed. Engl.* **1989**, *28*, 446.

[14] C. Mealli, A. Ienco, A. Poduska, R. Hoffmann, *Angew. Chem.* **2008**, *120*, 2906; *Angew. Chem. Int. Ed.* **2008**, *47*, 2864.

[15] R. Hoffmann, C. Mealli, S. Alvarez, essay to be published.

[16] V. Polo, J. Andrés, B. Silvi, *J. Comput. Chem.* **2007**, *28*, 857.

[17] B. Cordero, V. Gómez, A. E. Platero-Prats, M. Revés, J. Echeverría, E. Cremades, F. Barragán, S. Alvarez, *Dalton Trans.* **2008**, 2832.

[18] K. Fujisawa, Y. Moro-oka, N. Kitajima, *J. Chem. Soc. Chem. Commun.* **1994**, 623; M. E. Helton, D. Maiti, L. N. Zakharov, A. L. Rhenigold, J. A. Porco, Jr., K. D. Karlin, *Angew. Chem.* **2006**, *118*, 1156; *Angew. Chem. Int. Ed.* **2006**, *45*, 1138.

[19] A. L. Ma, J. B. Thoden, L. F. Dahl, *J. Chem. Soc. Chem. Commun.* **1992**, 1516.

[20] T. A. Albright, J. K. Burdett, M.-H. Whangbo, *Orbital Interactions in Chemistry*, John Wiley and Sons, New York, **1985**.

[21] A. J. Arce, P. Arrojo, A. J. Deeming, Y. De Sanctis, *J. Chem. Soc. Chem. Commun.* **1991**, 1491; C. A. Ghilardi, S. Midollini, A. Orlandini, G. Scapacci, *J. Chem. Soc. Dalton Trans.* **1992**, 2909.

[22] S. Alvarez, J. Cirera, *Angew. Chem.* **2006**, *118*, 3078; *Angew. Chem. Int. Ed.* **2006**, *45*, 3012.

[23] L. Han, L.-X. Shi, L.-Y. Zhang, Z.-N. Chen, M.-C. Hong, *Inorg. Chem. Commun.* **2003**, *6*, 281.

[24] Y.-H. Qin, M.-M. Wu, Z.-N. Chen, *Acta Crystallogr. Sect. A* **2003**, *59*, m317.

[25] N. P. Mankad, E. Rivard, S. B. Harkins, J. C. Peters, *J. Am. Chem. Soc.* **2005**, *127*, 16032.

[26] S. B. Harkins, N. P. Mankad, A. J. M. Miller, R. K. Szilagyi, J. C. Peters, *J. Am. Chem. Soc.* **2008**, *130*, 3478.

[27] Y. M. Rhee, M. Head-Gordon, *J. Am. Chem. Soc.* **2008**, *130*, 3878.

[28] K. B. Wiberg, F. H. Walker, *J. Am. Chem. Soc.* **1982**, *104*, 5239; P. Seiler, *Helv. Chim. Acta* **1990**, *73*, 1574.

[29] R. F. W. Bader, *Chem. Rev.* **1991**, *91*, 893; R. F. W. Bader, *Atoms in Molecules: A Quantum Theory*, Clarendon Press, Oxford, **1995**.

[30] R. Hoffmann, *Angew. Chem.* **1982**, *94*, 725; *Angew. Chem. Int. Ed. Engl.* **1982**, *21*, 711.

[31] B. Sigwarth, L. Zsolnai, H. Berke, G. Huttner, *J. Organomet. Chem.* **1982**, *226*, 5.

[32] M. J. Frisch, G. W. Trucks, H. B. Schlegel, G. E. Scuseria, M. A. Robb, J. R. Cheeseman, J. A. Montgomery, T. Vreven, K. N. Kudin, J. C. Burant, J. M. Millam, S. S. Iyengar, J. Tomasi, V. Barone, B. Mennucci, M. Cossi, G. Scalmani, N. Rega, G. A. Petersson, H. Nakatsuji, M. Hada, M. Ehara, K. Toyota, R. Fukuda, J. Hasegawa, T. Ishida, T. Nakajima, Y. Honda, O. Kitao, H. Nakai, M. Klene, X. Li, J. E. Knox, H. P. Hratchian, J. B. Cross, C. Adamo, J. Jaramillo, R. Gomperts, R. E. Stratmann, O. Yazyev, A. J. Austin, R. Cammi, C. Pomelli, J. Ochterski, P. Y. Ayala, K. Morokuma, G. A. Voth, P. Salvador, J. J. Dannenberg, V. G. Zakrzewski, S. Dapprich, A. D. Daniels, M. C. Strain, O. Farkas, D. K. Malick, A. D. Rabuck, K. Raghavachari, J. B. Foresman, J. V. Ortiz, Q. Cui, A. G. Baboul, S. Clifford, J. Cioslowski, B. B. Stefanov, G. Liu, A. Liashenko, P. Piskorz, I. Komaromi, R. L. Martin, D. J. Fox, T. Keith, M. A. Al-Laham, C. Y. Peng, A. Nanayakkara, M. Challacombe, P. M. W. Gill, B. Johnson, W. Chen, M. W. Wong, C. Gonzalez, J. A. Pople, Gaussian 03, Revision C.02, Gaussian Inc., Wallingford, CT, **2004**.

[33] A. D. Becke, *J. Chem. Phys.* **1993**, *98*, 5648.

[34] C. Lee, W. Yang, R. G. Parr, *Phys. Rev. B* **1988**, *37*, 785.

[35] A. Schäfer, C. Huber, R. Ahlrichs, *J. Chem. Phys.* **1994**, *100*, 5829.

[36] A. Schäfer, H. Horn, R. Ahlrichs, *J. Chem. Phys.* **1992**, *97*, 2571.

[37] C. Adamo, V. Barone, *Chem. Phys. Lett.* **2000**, *330*, 152; M. Cosi, V. Barone, *J. Phys. Chem. A* **1998**, *102*, 1995.
[38] E. Ruiz, P. Alemany, S. Alvarez, J. Cano, *J. Am. Chem. Soc.* **1997**, *119*, 1297; E. Ruiz, S. Alvarez, A. Rodríguez-Fortea, P. Alemany, Y. Pouillon, C. Massobrio, in *Magnetism: Molecules to Materials, Vol. 2* (Eds.: J. S. Miller, M. Drillon), Wiley-VCH, Weinheim, **2001**, p. 227; E. Ruiz, J. Cano, S. Alvarez, P. Alemany, *J. Comput. Chem.* **1999**, *20*, 1391.
[39] J. C. Ortiz, C. Bo, Departament de Química Física i Inorgànica (Universitat Rovira i Virgili), Tarragona (Spain), 1998.
[40] F. H. Allen, *Acta Crystallogr. Sect. A* **2002**, *58*, 380.
[41] ICSD, Gmelin-Institut für Anorganische Chemie and Fachinformationzentrum (FIZ), Karlsruhe, **1995**.

Received: May 13, 2008
Published online: November 21, 2008

